Scaling of Spoke Rotation Frequency within a Penning Discharge & Code Development Updates

IEPC-2019-816

Presented at the 36th International Electric Propulsion Conference
University of Vienna, Austria
September 15-20, 2019

Andrew T. Powis*
Princeton University, Princeton, New Jersey, 08544, USA

Johan A. Carlsson†, Igor D. Kaganovich‡, Eduardo Rodriguez§ and Yevgeny Raitses¶
Princeton Plasma Physics Laboratory, Princeton, New Jersey, 08540, USA

and

Andrei Smolyakov‖
University of Saskatchewan, Saskatoon, Saskatchewan, S7N 5E2, Canada

A rotating plasma spoke is shown to develop in two-dimensional full-sized kinetic simulations of a Penning discharge cross-section. Similarity between collisional and collisionless simulations demonstrates that ionization is not necessary for spoke formation. Parameter scans with discharge current I_d, applied magnetic field strength B and ion mass m_i show that spoke frequency scales with $\sqrt{eE_rL_n/m_i}$, where E_r is the radial electric field, L_n is the gradient length scale and e is the fundamental charge. This scaling suggests that the spoke may develop as a non-linear phase of the collisionless Simon-Hoh instability.

A new code is designed, incorporating high-performance-computing best practices with the goal of performing un-scaled simulations of anomalous transport within E×B discharges. Tests against a known benchmark demonstrate good weak scaling behaviour, and further demonstrate that large simulation domains are necessary to capture the complete physics of the system.

*PhD Candidate, Department of Mechanical and Aerospace Engineering, apowis@princeton.edu
†Computational Physicist, Computational Plasma Physics Group, carlsson@radiasoft.net
‡Principal Research Physicist, Plasma Science and Technology Department, ikaganov@pppl.gov
§PhD Candidate, Program in Plasma Physics, erodrigu@pppl.gov
¶Principal Research Physicist, Plasma Science and Technology Department, yraitses@pppl.gov
‖Professor, Department of Physics and Engineering Physics, andrei.smolyakov@usask.ca

Nomenclature

r = Radial coordinate in cylindrical geometry
θ = Azimuthal coordinate in cylindrical geometry
z = Axial coordinate in cylindrical geometry
$\mathbf{B}$ = Magnetic field vector
$\mathbf{B}_r$ = Radial magnetic field vector
$\mathbf{B}_z$ = Axial magnetic field vector
B = Magnetic field magnitude
B_0 = Applied (external) magnetic field magnitude
$\mathbf{E}$ = Electric field vector
$\mathbf{E}_r$ = Radial electric field vector
$\mathbf{E}_\theta$ = Azimuthal electric field vector
E_r = Radial electric field magnitude
L_n = Radial gradient length scale
e = Fundamental charge
U_{ion} = Ionization energy
m_s = Mass of species s
n_s = Number density of species s
n_0 = Plasma number density
I_d = Discharge current
I_s = Injection current of species s
T_s = Temperature of species s
$T_{s,inj}$ = Injection temperature of species s
V_b = Electron beam injection energy
P_n = Neutral gas pressure
ε_r = Relative permittivity
R_0 = Penning discharge radius
R_i = Injection radius
σ_{en} = Electron-neutral collision cross-section
Δx = Cell edge length
Δt = Time step size
f_s = Measured frequency
$f_{s,th}$ = Predicted frequency
$\omega_{s,th}$ = Predicted angular frequency
k = Wavenumber
k_θ = Azimuthal wavenumber
v_r = Rotation speed
v_s = Ion-acoustic speed
v_0 = $\mathbf{E} \times \mathbf{B}$ drift speed
v_* = Diamagnetic drift speed
v_{civ} = Critical ionization speed
L_x = Reference azimuthal length
E_y = Axial electric field magnitude (for Hall thruster simulations)

I. Introduction

Hall plasmas, consisting of magnetized electrons and unmagnetized ions, exhibit a wide range of plasma instabilities.[1,2] In some systems these instabilities may result in the formation of a long wavelength, low frequency fluctuation in plasma density, propagating in the $\mathbf{E} \times \mathbf{B}$ direction. This rotating structure is commonly referred to as a plasma "spoke".

The spoke has been well characterized within a number of experimental devices, including Hall thrusters,[3–15] planar magnetrons,[16–23] cylindrical magnetrons[24,25] and Penning discharges.[26–28] These devices feature cylindrical geometry, with electron drift and spoke propagation occurring in the azimuthal direction.

The plasma spoke may play an important role in the anomalous transport of electrons across the applied magnetic field, a source of reduced efficiency.[29] Using separated probes within a Hall thruster, Janes & Lowder[3] measured an azimuthal electric field correlated with the passage of the spoke and suggested that the resulting $\mathbf{E}_\theta \times \mathbf{B}_r$ drift was enhancing electron transport towards the thruster anode. More recently, the use of segmented anodes within a Cylindrical Hall Thruster[30] demonstrated that half of the discharge current was being carried through the spoke, evidence for enhanced transport through the structure.[6,8]

Due to its highly non-linear, turbulent and global nature, the spoke has continued to evade a clear theoretical understanding. Proposed mechanisms include a type of ionization wave,[3] whereby the azimuthal field at the front of the spoke provides sufficient energy to accelerate electrons and ionize neutrals, propagating the plasma density perturbation. The ionization wave would progress at the Critical Ionization Velocity (CIV)[31] defined as $v_{civ} = \sqrt{2U_{ion}/m_n}$, where U_{ion} and m_n are the ionization energy and mass of the neutral species respectively.

Alternatively, the spoke may be the result of collective effects, with the Collisionless Simon-Hoh Instability (CSHI) being a likely candidate.[26,27] Charge separation between drifting electrons and unmagnetized (non-drifting) ions generates an azimuthal electric field. If the background electric field and density gradients within the system are aligned $\mathbf{E}_0 \cdot \nabla n_0 > 0$, then the the resulting azimuthal field will act to enhance perturbations in plasma density, driving the instability.

Investigation of the plasma spoke within a Penning discharge offers several advantages, most immediately being improved access for diagnostics. The applied magnetic field is ideally uniform and aligned with the axis of the device, allowing the electron dynamics parallel to the device axis to be decoupled from those in the transverse direction. For purposes of simulations and theory, the system can therefore be treated as approximately two-dimensional. The lack of a magnetic field gradient reduces the number of energy sources for instabilities, eliminating possible driving mechanisms for spoke formation. In many systems the plasma is also weakly collisional, further simplifying theoretical considerations. This makes it an ideal system within which to study spoke formation and anomalous transport.

Simulations have played an increasingly important role in understanding the formation of the spoke and its connection to anomalous transport. Kinetic techniques are required to self-consistently capture transport effects, with the Particle-in-Cell Monte-Carlo Collision (PIC-MCC) method commonly being used. The challenge with PIC-MCC comes from the numerical requirement to resolve the smallest time and length scales associated with the plasma, the electron plasma frequency and Debye length respectively. These constraints result in a significant computational overhead required to capture the vastly multi-scale physics observed within devices such as the Penning discharge.

This challenge is usually dealt with in one of two ways. The first approach is to scale the system in some way, either by reducing device size (to reduce the number of cells), decreasing the plasma density or increasing the relative permittivity (to increase the Debye length and therefore allowable cell size). With improving computational capabilities and employing scaling it has become possible to simulate 2D profiles of a device,[32–39] and even 3D devices.[40–43] Low mode number, rotating structures have been observed in a number of these simulations, in particular, Matyash found close agreement between the frequency of the rotating structure observed within a model of a wall-less Hall thruster[44] and experiments at CRNS.[45]

The second technique adopts a hybrid approach, modeling electrons as a fluid, such that the associated length and time scales need not be resolved. The primary disadvantage of this technique is that kinetic electron transport effects are not captured self-consistently and must be incorporated via a model informed from experimental evidence. None-the-less, hybrid models have had success in reproducing the spoke. Most recently a two-dimensional axial-azimuthal hybrid code captured the motion of the spoke within a simulated thruster channel with SPT-100 like parameters.[46] The spoke velocity was on the order of what has previously been observed in experiments, and suggested to be the result of an instability driven by magnetic field and density gradients.[4,47]

Despite these capabilities, work is still in progress to produce unscaled, fully kinetic simulations of entire devices. Perhaps equally as challenging will be developing tools for analysing the enormous amount of data produced by such simulations.

The present paper summarises the results of our recent publication,[48] whereby scaling of the spoke frequency was studied within two-dimensional PIC-MCC simulations of a Penning discharge with scaled relative permittivity. We then proceed to discuss development of new computational tools for the unscaled modeling of the Penning discharge or Hall thruster channel. These tools will be applied to the study of anomalous cross-field transport over the multi-scale phenoma encapsulated within low-temperature plasma turbulence and through the emergence of coherence structures such as the plasma spoke.

II. Methodology

The scaling of spoke frequency was studied using the Large-Scale Plasma code (LSP).[49] LSP is a multi-purpose and versatile PIC code, widely benchmarked and validated within the community.[49–52] It was assumed that the system could be treated electrostatically, and Poisson's equation inverted to obtain the electric potential from charge density. PPPL modifications to the code[53] include incorporation of the latest version of the Portable Extensible Toolkit for Scientific Computation (PETSc)[54–56] for improved performance and scalability. Poisson's equation was inverted via the SuperLU,[57,58] LU factorization package accessed via the PETSc interface.

Simulation were modeled off the Penning discharge experiment at the PPPL-HTX laboratory.[28] Within this device an RF plasma cathode injects electrons along the axial magnetic field, ionizing a low pressure gas of either Argon or Xenon. Electron motion in the radial direction is inhibited by an axially applied uniform magnetic field. Ions are weakly magnetized and therefore significantly more mobile, giving rise to an ambipolar radial electric field. The applied magnetic field and ambipolar electric field result in electrons undergoing $\mathbf{E}_r \times \mathbf{B}_z$ drifts in the azimuthal direction. The plasma is surrounded by a grounded cylindrical metal anode with 10 cm diameter. The ends of the cylinder are dielectric, preventing the short-circuit effect. The device geometry and simulation geometry are shown in Figure 1.

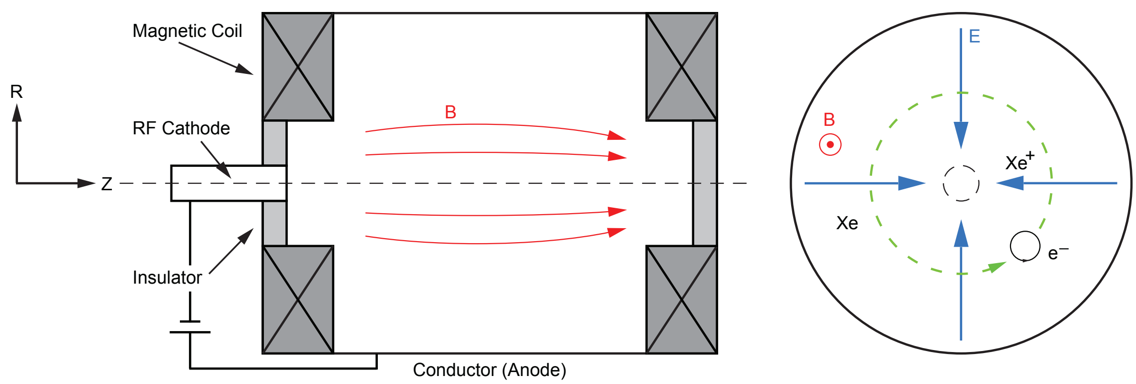

Figure 1: a) Experimental setup of the Penning discharge at PPPL[28] in r-z geometry. Magnetic field lines are indicated in red. b) Cross-section of the Penning discharge, representative of the simulation domain in r-θ geometry. Blue lines indicate the radial ambipolar electric field and green-dashed lines represent the direction of the electron $\mathbf{E} \times \mathbf{B}$ drift. Xenon ions are unmagnetized.

A slice of the device cross-section was modeled on a uniform Cartesian grid, with particles evolving in 2D-3V phase space. While a two-dimensional model appears to be a good approximation for this system, a limit of these simulations is that they will not capture axial modes or the effects of the dielectric end plates. A Cartesian grid was chosen over a cylindrical grid to avoid numerical instabilities associated with the grid singularity at zero radius.

A uniform magnetic field is applied perpendicular to the simulation domain. To shed light on the formation mechanism of the spoke, both collisionless and collisional simulations were performed. In collisionless simulations, electrons and ions are injected into the center of the trap at fixed current and initial temperature, I_e, $T_{e,inj}$ and I_i, $T_{i,inj}$ respectively (see Table 1). For collisional simulations, electrons with energy V_b are injected into a uniform background of neutrals with pressure P_n and temperature T_n (see Table 1), and ions form via ionization. Modeled collisions include Coulomb collisions between all charged species and electron-neutral collisions. Neutral particle excitation was not modeled. Both electron-neutral elastic and ionizing collisions were informed by experimental data.[59]

Table 1: Physical parameters of simulations.

Property	Symbol	Value	Units
Relative Permittivity	ε_r	400	–
Discharge Radius	R_0	2.5	cm
Injection Radius	R_i	0.1	cm
Applied Magnetic Field	B_0	100	$Gauss$
Electron Current	I_e	250	mA
Ion Current	I_i	100	mA
Discharge Current	I_d	-150	mA
Electron Injection Temperature	$T_{e,inj}$	5	eV
Ion Injection Temperature	$T_{i,inj}$	293	K
Electron Beam Energy	V_b	15	eV
Neutral Pressure	P_n	1	$mTorr$
Neutral Temperature	T_n	293	K
Electron-Neutral Cross-Section	σ_{en}	2.88×10^{-19}	m^2

Simulations were designed to be completed within a realistic time frame, enabling parametric investigations of instabilities within the Penning discharge. To achieve this goal the simulation domain was reduced from 10 cm to 5 cm and the Xenon gas mass was reduced to that of Helium-4. To relax the strict constraints on PIC simulations the relative permittivity was increased to $\varepsilon_r = 400$, increasing the Debye length and reducing plasma frequency, thereby allowing for larger cell size and time step respectively. The relative permittivity was scaled, since it is suspected to play a small role in the instabilities which may be responsible for spoke formation. This scaling, however, will influence higher frequency instabilities, which may effect the cross-field transport rate of the plasma.

These modifications led to a grid of 250×250 cells, with cell edge length $\Delta x = 200\ \mu m$ and time step $\Delta t = 40\ ps$, suitable to resolve all relevant plasma length and time scales. Simulations of 100 μs of plasma time could therefore be completed within 2 days. Simulation were run with 28 cores on the Princeton University Perseus supercomputer and 24 cores on the Department of Energys National Energy Research Scientific Computing Center (NERSC) Edison supercomputer. Post-processing was performed via the IDL based LSP post-processing tool P4 and in-house *Python* codes.

III. Results & Discussion

A. Comparing Collisionless and Collisional Simulations of the Rotating Spoke

For collisionless simulations, electrons and ions are injected into the center of an initially empty domain. The negative discharge current $I_d = I_i - I_e < 0$, results in an initially non-neutral plasma until sufficient ions have been injected to provide a neutralizing background. Quasi-neutrality is achieved around 100 μs, after which a long-wavelength, single mode structure forms, rotating in the azimuthal direction. When viewed in the direction of the applied magnetic field, the structure rotates anti-clockwise.

Figure 2 shows contour plots of instantaneous electron density, plasma potential, and current streamlines, commencing at 250 μs and incremented by a $\pi/4$ phase shift of the rotating structure. The phase of the rotating structure is measured to obtain a rotation frequency of $f_s = 66.0\ kHz$, significantly lower than the electron and ion plasma frequencies, the electron cyclotron frequency and the lower-hybrid frequency. When computed at $r = R_0/2$, the structure rotation speed is $v_r = 5.18\ km/s$, around half of the ion-acoustic speed $v_s = 10.6\ km/s$.

Numerical convergence was verified by measuring the mode frequency for simulations with half the cell size, half the time step and double the particle number, showing no more than a 3.8% discrepancy. Modeling convergence was checked by scaling the relative permittivity, which for $\varepsilon_r = 100$ agrees within 11 %.

In collisional simulations, electrons are injected into a neutral background gas, the system rapidly reaches quasi-neutrality from ions formed via ionization. A large scale, low-frequency single mode develops after 20 μs. Figure 3 shows four contour plots of electron density, commencing at 61.4 μs and incremented by a $\pi/4$ phase shift of the rotating structure.

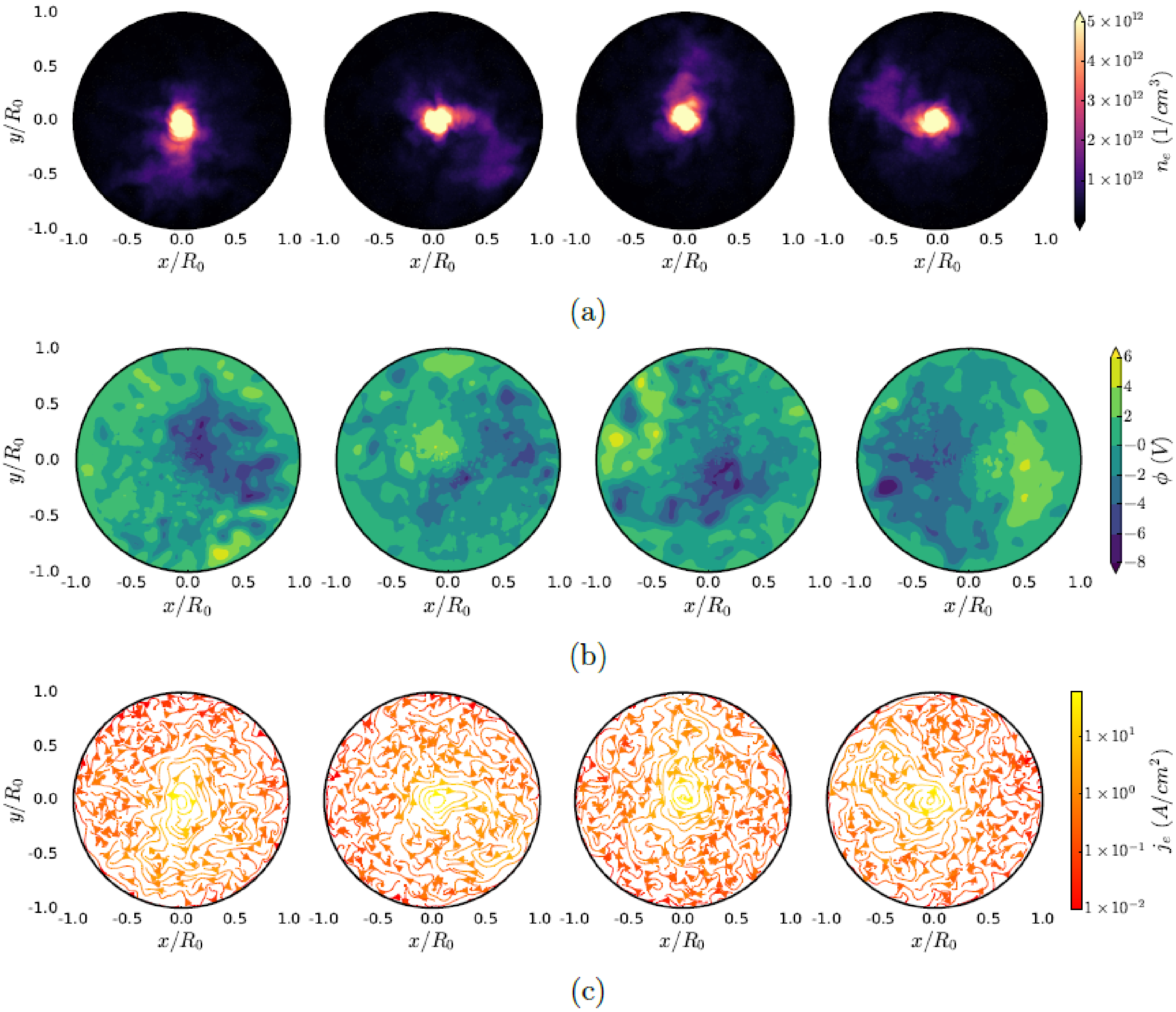

Figure 2: a) Electron density contours, b) plasma potential contours, c) current streamlines, of the collisionless Penning discharge at simulation time, from left to right; 250 μs, 253.8 μs, 257.5 μs and 261.3 μs. An animated version of part a) of this figure is available at https://youtu.be/sM1X637YAqM.

The spoke frequency is computed as $f_s = 62.4\ kHz$ with a rotation speed at $r = R_0/2$ of $v_r = 4.90\ km/s$, both within 6% of the values obtained for the collisionless case. The structure of the density contours reveal similar behaviour to that of the collisionless case, although the spoke structure extends further towards the anode and appears to have a larger azimuthal extent. This most likely indicates that ionization is occurring not only within the injection region at the center of the trap, but also within the spoke itself, enhancing plasma density and broadening the spoke.

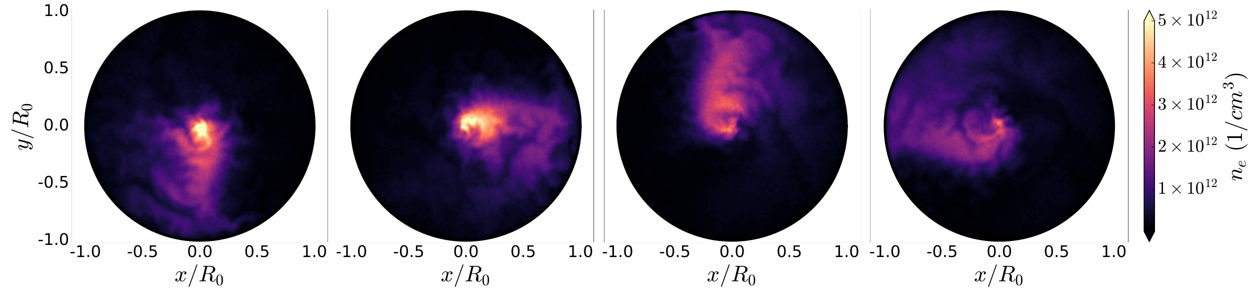

Figure 3: Electron density contours of the collisional Penning discharge at simulation times, from left to right; 61.4 μs, 65.8 μs, 70.7 μs and 74.2 μs. An animated version of this figure is available at https://youtu.be/Dv88TRtVxFk.

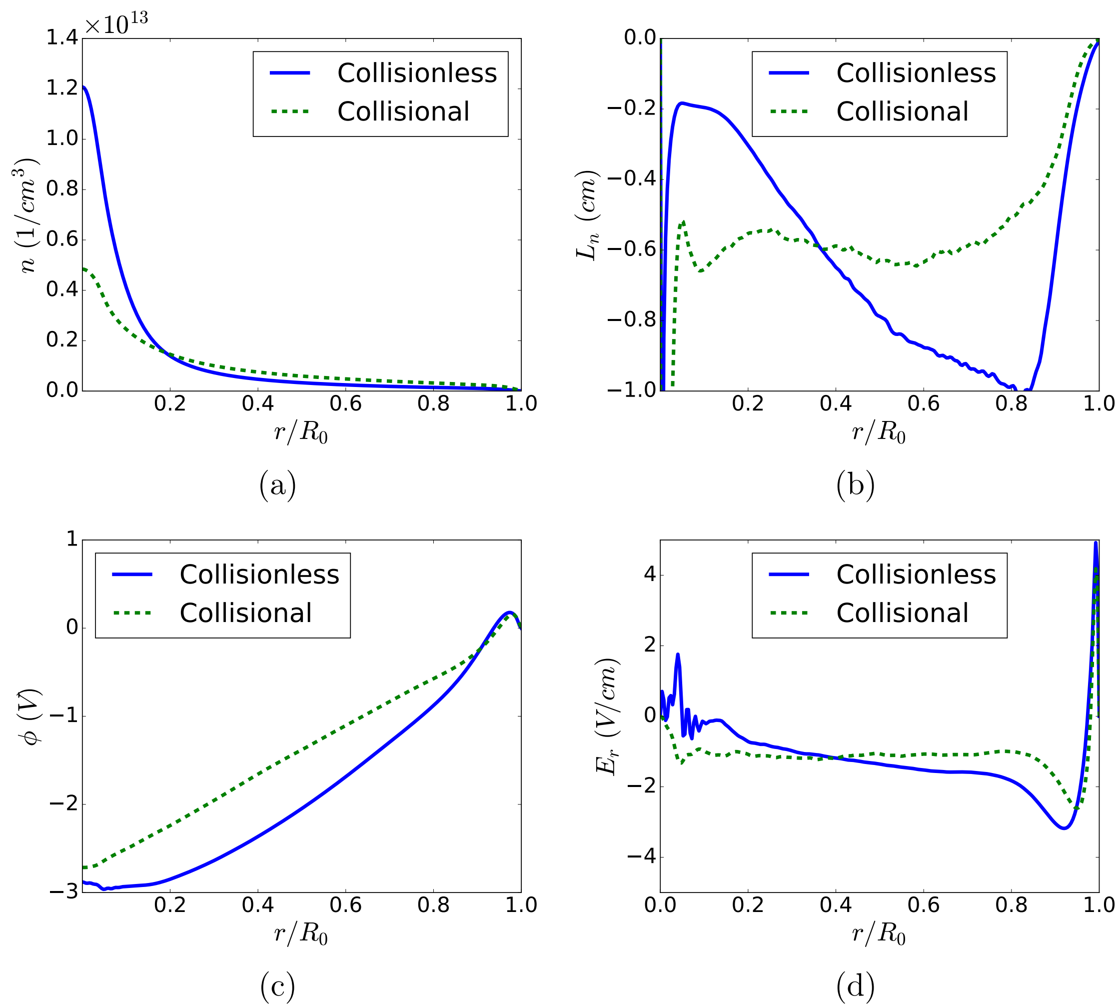

Figure 4: Azimuthally and temporally averaged radial profiles of a) electron density $n_e(r)$, b) gradient-length-scale $L_n(r) = n_e(r)/(dn_e(r)/dr)$, b) electric potential $\phi(r)$, c) radial electric field $E_r(r)$ for collisional and collisionless cases.

The average radial density, gradient length scale, electric potential and electric field profiles (see Figure 4) are computed over numerous spoke rotation frequencies after each simulation achieves quasi-steady state. The density profile and density gradients for the collisional case are shallower than the collisionless case.

This also indicates that ionization is likely occurring outside of the injection region, since a more diffuse source of ions can sustain a flatter electron density profile. The electric potential and electric field profiles are similar between both cases, with the collisional case exhibiting a linear potential and therefore flatter electric field profile.

Estimates for the $\mathbf{E} \times \mathbf{B}$ and diamagnetic drift speeds for the collisionless case are obtained by averaging the radial electric field and gradient length scales away from the injection and sheath regions within $r \in [0.2R_0, 0.8R_0]$, giving an average azimuthal $\mathbf{E} \times \mathbf{B}$ speed of $v_0 = \langle |E_r| \rangle / B_0 = 13.1\ km/s$ and electron diamagnetic drift speed of $v_* = T_e/(e \langle |L_n| \rangle B_0) = 64.5\ km/s$. Within the same frame of reference as Figure 2, both of these drifts occur in the anti-clockwise direction. The rotation speed of the large scale structure is an order of magnitude smaller than the electron diamagnetic drift speed and less than half of the $\mathbf{E} \times \mathbf{B}$ speed. In both cases, since the large scale structure is shown to be low-frequency, long-wavelength and rotating in the $\mathbf{E} \times \mathbf{B}$ direction it exhibits all of characteristic behaviour of the plasma spoke, as observed within the Penning discharge and numerous other experiments.[3,5,7,28] Therefore it is proposed that the rotating structure observed within these simulations is the plasma spoke.

Despite small quantitative differences, the spoke frequency and structure as well as the average discharge profiles are remarkably similar between the collisional and collisionless cases. This indicates that the same fundamental mechanism is likely responsible for the formation of the spoke. Since it is shown by the collisionless case that ionization is not necessary for spoke formation, it is unlikely that the spoke is caused by an ionization wave. Furthermore, for reduced mass Xenon, the CIV[31] $v_{civ} = 17.1\ km/s$ is significantly larger than the spoke rotation speed.

This leaves the Collisionless Simon-Hoh Instability (CSHI) as a likely candidate for the formation of the spoke within these simulations. In both the collisional and collisionless cases $E_r(r)/L_n(r) > 0\ \forall\ r$ such that the instability criterion for the CSHI is satisfied. Keeping in mind the limitations of these simulations it is therefore possible that the rotating spoke observed within the Penning discharge is the result of the CSHI, rather than an ionization wave.

B. Spoke Frequency Scaling with Discharge Parameters

Considering the relative magnitudes of the average diamagnetic drift speed $v_* = 64.5\ km/s$, $\mathbf{E} \times \mathbf{B}$ speed $v_0 = 13.1\ km/s$ and ion-sound speed $v_s = 10.6\ km/s$, linear CSHI theory suggests the following scaling for the spoke frequency,[60]

$$\omega_{s,th} = \sqrt{\frac{v_s^2 v_0}{v_*} k^2} = \sqrt{\frac{eE_r L_n}{m_i} k^2}. \tag{1}$$

Assuming a single azimuthal mode propagating at $r = R_0/2$, we have $k = k_\theta = 2/R_0$, and therefore a theoretical estimate for the spoke frequency,

$$f_{s,th} = \frac{1}{\pi R_0} \sqrt{\frac{eE_r L_n}{m_i}}. \tag{2}$$

The validity of this scaling is tested by modifying the discharge parameters of the collisionless simulation. For each simulation, the radial electric field multiplied by the gradient length scale $\langle |E_r L_n| \rangle$ is averaged for $r \in [0.2R_0, 0.8R_0]$. The estimate for spoke frequency $f_{s,th}$ is plotted with the measured spoke frequency f_s for different discharge parameters.

Figure 5a demonstrates a correlation between spoke frequency and discharge current magnitude. Increasing the applied magnetic field strength reduces electron mobility and therefore results in an enhanced ambipolar electric field. Therefore, as per Equation 2, the spoke frequency should scale as $f_s \sim \sqrt{B}$. This is demonstrated in Figure 5b and consistent with experimental observations.[28] Ion-mass m_i is varied and Figure 5c shows a near linear correlation between spoke frequency and $1/\sqrt{m_i}$ (normalized to the ion mass of Helium-4), consistent with experimental observation.[28] This also demonstrates that the spoke rotation velocity scales in an identical way to the ion-acoustic velocity with respect to ion-mass.

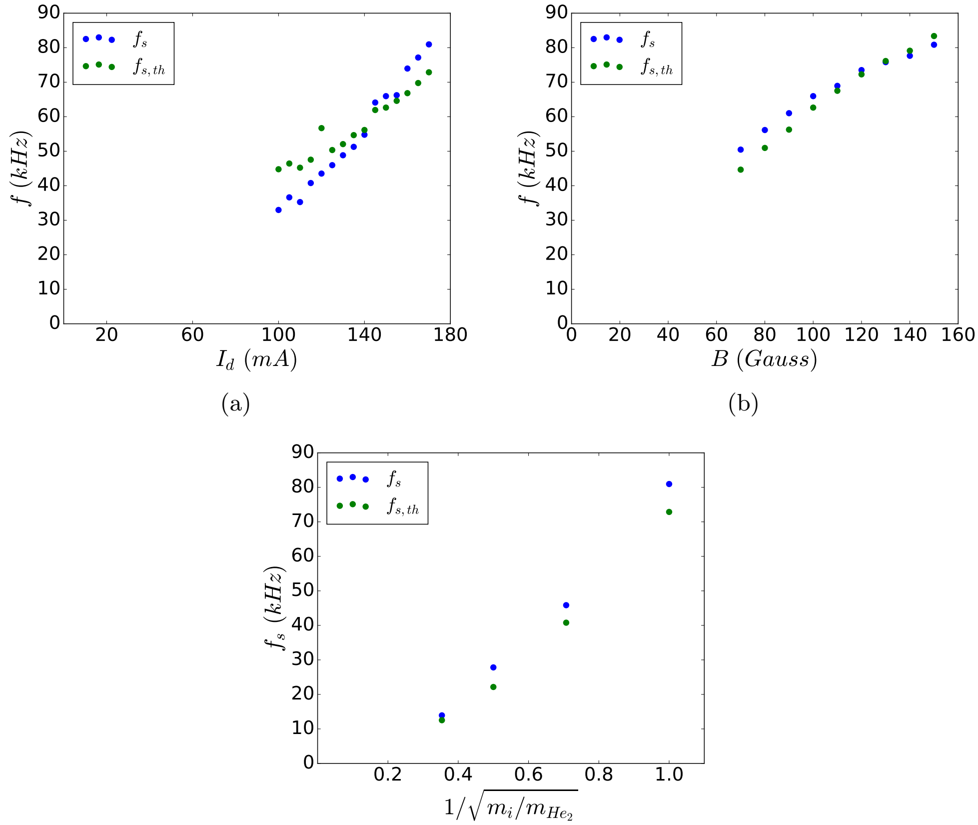

(a)

(b)

(c)

Figure 5: Spoke rotation frequency f_s and predicted rotation frequency $f_{s,th}$ as a function of; (a) discharge current magnitude I_d, (b) applied magnetic field strength B, (c) inverse square root of ion mass m_i.

For each of these parameter scans the approximate theoretical estimate for the spoke frequency shows good agreement in both magnitude and scaling to the measured numerical spoke frequency, providing strong evidence for this scaling relationship and that the CSHI is the driving instability of the rotating spoke. It should be taken into consideration that the observed structure is clearly highly non-linear and turbulent, making it surprising that a simple estimate based on linear theory provides such an accurate fit.

IV. Code Development for Modeling Anomalous Transport

Figure's 2a and 3 as well as their corresponding animations (see links in Figure captions), show that the spoke does not appear to rotate as a rigid body, but rather as a density perturbation rich in micro-structure. This is further evidenced by Figure 2b which shows a noisy and highly fluctuating plasma potential, with dips in plasma potential only weakly correlated with the passage of the spoke. Figure's 2b and 2c show that there is neither a strong electric potential gradient nor current channel associated with the front of the spoke, however both indicate the presence of a turbulent plasma. Qualitatively it appears that any increase in cross-field electron transport within the structure will be the result of enhanced turbulence, rather than strong correlation with the azimuthal electric field.

While scaling of the relative permittivity ϵ_r is predicted to have little effect on the global spoke structure, it will likely influence the micro-structure developing within the spoke. This will limit the accuracy of any study which aims to develop an understanding of these structures, or predict the resulting rates of transport. It is therefore necessary to develop simulation tools which can fully resolve the physics of the Penning discharge, or equivalent system such as a Hall thruster channel.

We seek to push the boundaries for low-temperature plasma simulations, by developing the framework for a high performance kinetic particle-in-cell code. This code is written from the ground up to be scalable to many thousands of processors, and draws on lessons learned from the plasma community in developing simulation packages for high-temperature plasma applications such as fusion and laser-plasmas.[61,62] This framework features multi-level parallelism via MPI, OpenMP and vectorization, as well as mixed domain and particle list decomposition to optimally distribute resources based on the physics of the system under investigation.

As stated above, a critical challenge for kinetic simulations is the requirement to resolve the plasma Debye length. This is particularly challenging for low-temperature plasmas, where the Debye length can be three or more orders of magnitude smaller than the system size, necessitating the use of very fine grids. Many low-temperature systems can be treated accurately using the electrostatic approximation, which removes the constraint of resolving the CFL condition for the speed of light, although introduces a challenge in solving an elliptical equation over enormous grid domains. Solvers must also be robust, in the sense that they should be able to handle complex geometry and boundary conditions such as conducting, dielectric and free-exit boundaries. In the past decade, several high-performance and scalable packages have emerged for solving such systems centered around multi-grid techniques.[54,63,64] These capabilities effectively overcome these challenges and enable electrostatic systems to be solved, in a scalable way, on the very large grids required.

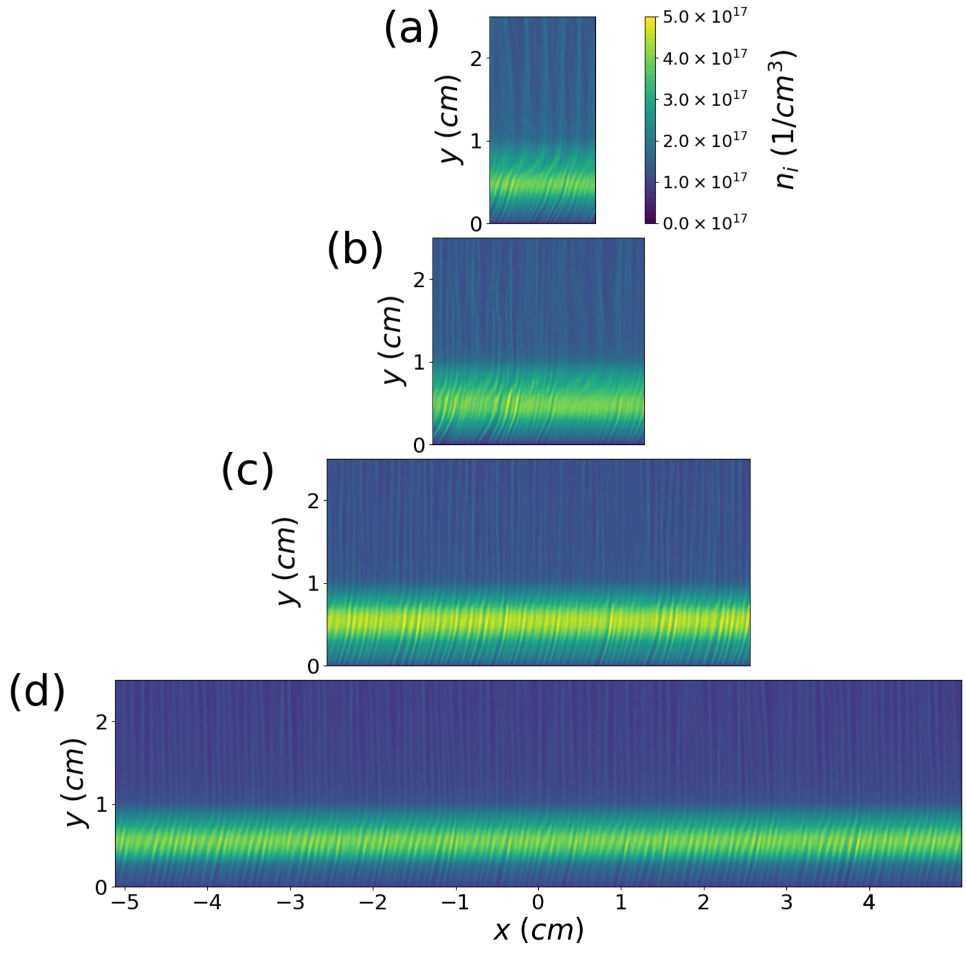

Figure 6: Contour plots of ion density within simulations of a Hall thruster channel, similar to those described in Boeuf & Garrigues.[65] The azimuthal extend of the simulation domain is adjusted from (a) $L_x = 1.28\ cm$ to (b) $2L_x = 2.56\ cm$, (c) $4L_x = 5.12\ cm$ and (d) $8L_x = 10.24\ cm$.

Besides implementation of these techniques,[63] the code relies on tried and tested particle-in-cell algorithms. Particles are pushed in double precision via the standard Boris algorithm.[66] Random numbers are generated via the thread safe SIMD oriented Fast Mersenne Twister (dSFMT) package.[67] Rather, significant effort was placed on incorporating these algorithms, particle boundaries, sources and sinks, and differentiation in the most scalable manor possible.

The new code was recently benchmarked as part of a global effort to demonstrate convergence between low-temperature plasma codes designed for the modeling of $\mathbf{E} \times \mathbf{B}$ discharges (see poster by T. Charoy in the proceedings of this conference). The simulation is similar to that of Boeuf & Garrigues[65] modeling a 2D-3V azimuthal segment of a Hall thruster channel. The setup is idealized in the sense that there are no collisions, and ionization as well as a virtual cathode are modeled via particle injection profiles. Simulations performed with the new code were in close agreement with the six other international codes benchmarked in the effort. Importantly, the code also demonstrated high speed as well as favourable weak scaling performance with particle number.

We extended the work of this benchmarking effort by studying the influence of azimuthal length of the Hall thruster segment on the averaged profiles of the discharge. Figure 6 shows contours of ion density after 20 μs of simulation time for the benchmarked azimuthal length ($L_x = 1.28\ cm$) and for lengths $2L_x$, $4L_x$ and $8L_x$ respectively. We see the emergence of similar instabilities as in the benchmarked case, although with a corresponding increase in wave peaks with azimuthal length. The instabilities appear qualitatively similar among the simulations, however the average axial profiles (between $16 - 20\ \mu s$) of ion density, axial electric field, and electron temperature (see Figure 7) show that there are underlying differences. Particularly curious is the increase in electron temperature for the simulation with $8L_x$ extent.

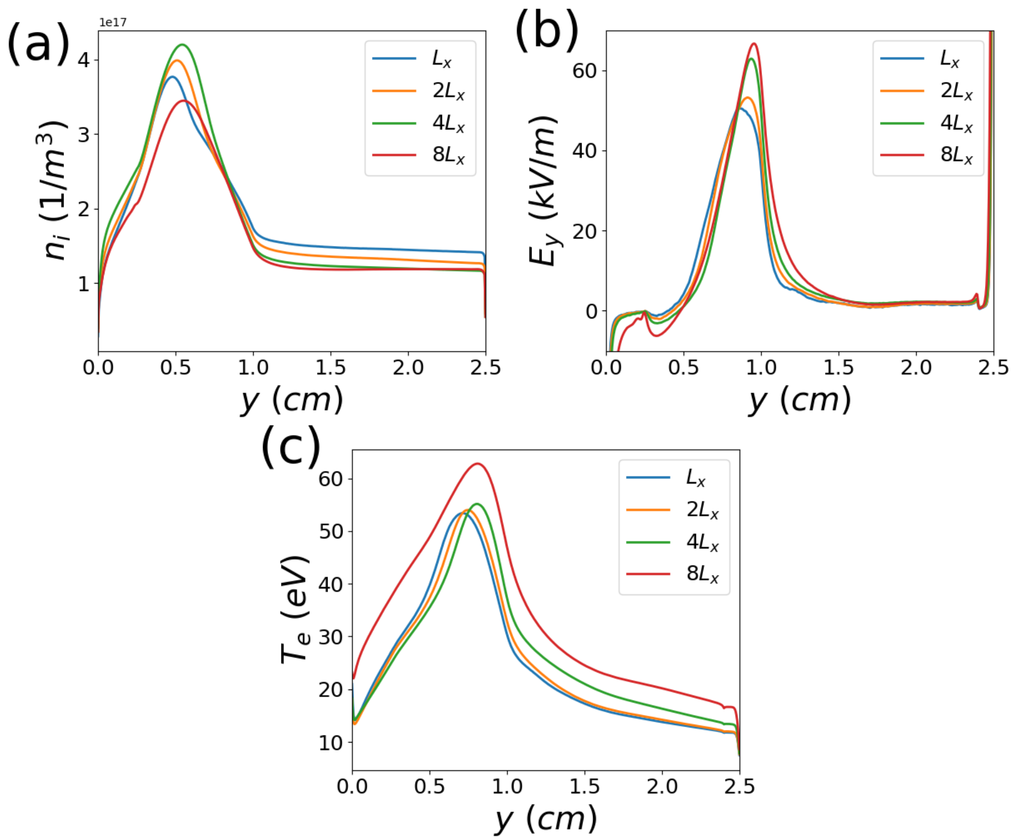

Figure 7: Azimuthally averaged axial profiles of (a) ion density n_i, (b) axial electric field E_y, and (c) electron temperature T_e within Hall thruster channel simulations of various azimuthal extends.

These changes in average axial behaviour could be due to several reasons. Possible explanations include the emergence of long-wavelength instabilities, not yet observable within the plots of ion density shown in Figure 6. Or more likely, 20 μs is simply not enough time for these larger simulations to reach steady state. While extended simulations of these larger domains are ongoing, it is clear that codes which can capture the entire domain of a device are important for fully resolving the physics, even for such an idealized simulation setup.

These simulations also provide an excellent opportunity to demonstrate the weak scaling behaviour of the new code. Figure 8 shows the average total time (in ms) per simulation step and the average time per step for critical code routines. The scaling was performed for simulations with azimuthal extents $\{0.25L_x, 0.5L_x, L_x, 2L_x, 4L_x, 8L_x, 16L_x\}$ with the largest simulation comprising a fully resolved kinetic simulation of a two-dimensional domain 20.48 $cm \times 2.5$ cm. We observe excellent weak scaling, demonstrating that two-dimensional simulations of a full Hall thruster channel are indeed made possible through the implementation of high-performance computing best practices.

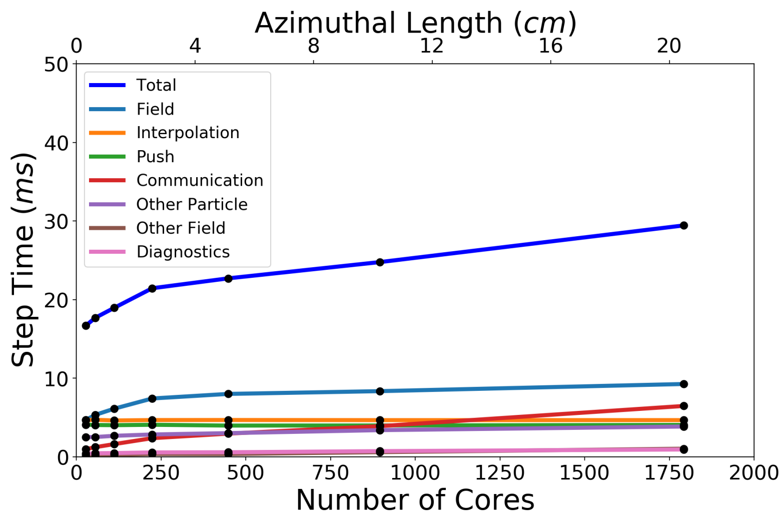

Figure 8: Results of weak scaling test for two-dimensional simulations of a Hall thruster channel. Step time's are measured in milliseconds and averaged over 1000 steps.

V. Conclusions

A highly non-linear turbulent structure rotating in the azimuthal $\mathbf{E} \times \mathbf{B}$ direction is observed to form within full-size two-dimensional kinetic simulations of a Penning discharge. This structure exhibits characteristic behaviour very similar to that of the rotating spoke observed in experiments. Similarity between simulations with and without ionization suggests that the spoke is not the result of an ionization wave. The generated ambipolar electric field and density gradient are aligned so as to destabilize the collisionless Simon-Hoh instability. The correlation of the resulting spoke frequency with the average radial electric field, gradient length scale and ion mass supports the claim that the collisionless Simon-Hoh instability is responsible for its formation.

A new code has been designed to study the effects of anomalous transport within $\mathbf{E} \times \mathbf{B}$ discharges. Emphasis was placed on adopting high-performance-computing best practices, to enable scalability up to thousands of cores and therefore simulations of very large domains. The code was shown to possess good weak scaling behaviour, and demonstrated that even within idealised simulations of a Hall thruster channel, the resolution of large length scales is critical to fully resolve the physics.

Acknowledgments

Physics work was supported by the Air Force Office of Scientific Research.

Code development was supported by the Princeton University Program in Plasma Science and Technology.

This research used resources of the National Energy Research Scientific Computing Center, a DOE Office of Science User Facility supported by the Office of Science of the U.S. Department of Energy under Contract No. DE-AC02-05CH11231.

This research used resources of the Perseus cluster at the TIGRESS high performance computer center at Princeton University, which is jointly supported by the Princeton Institute for Computational Science and Engineering and the Princeton University Office of Information Technology's High Performance Research Computing Center.

References

[1]E. Choueiri, “Plasma oscillations in hall thrusters,” *Physics of Plasmas*, vol. 8, no. 4, pp. 1411–1426, 2001.

[2]E. Chesta, C. M. Lam, N. B. Meezan, D. P. Schmidt, and M. A. Cappelli, “A characterization of plasma fluctuations within a hall discharge,” *IEEE transactions on plasma science*, vol. 29, no. 4, pp. 582–591, 2001.

[3]G. Janes and R. Lowder, “Anomalous electron diffusion and ion acceleration in a low-density plasma,” *The Physics of Fluids*, vol. 9, no. 6, pp. 1115–1123, 1966.

[4]Y. B. Esipchuk, A. Morozov, G. Tilinin, and A. Trofimov, “Plasma oscillations in closed-drift accelerators with an extended acceleration zone,” *Soviet Physics Technical Physics*, vol. 18, p. 928, 1974.

[5]J. Parker, Y. Raitses, and N. Fisch, “Transition in electron transport in a cylindrical hall thruster,” *Applied Physics Letters*, vol. 97, no. 9, p. 091501, 2010.

[6]L. Ellison, Y. Raitses, and N. J. Fisch, “Direct measurement of spoke-induced, cross-field electron transport in a cylindrical hall thruster,” in *IEPC-2011-173 Presented at the 32nd International Electric Propulsion Conference*, 2011.

[7]M. S. McDonald and A. D. Gallimore, “Rotating spoke instabilities in hall thrusters,” *IEEE Transactions on Plasma Science*, vol. 39, no. 11, pp. 2952–2953, 2011.

[8]C. Ellison, Y. Raitses, and N. Fisch, “Cross-field electron transport induced by a rotating spoke in a cylindrical hall thruster,” *Physics of Plasmas*, vol. 19, no. 1, p. 013503, 2012.

[9]M. E. Griswold, C. Ellison, Y. Raitses, and N. Fisch, “Feedback control of an azimuthal oscillation in the e× b discharge of hall thrusters,” *Physics of Plasmas*, vol. 19, no. 5, p. 053506, 2012.

[10]Y. Raitses, M. Griswold, L. Ellison, J. Parker, and N. Fisch, “Studies of rotating spoke oscillations in cylindrical hall thrusters,” in *48th AIAA/ASME/SAE/ASEE Joint Propulsion Conference & Exhibit*, p. 4179, 2012.

[11]D. Liu, R. E. Huffman, R. D. Branam, and W. A. Hargus, “Ultrahigh speed images of hall thruster azimuthal instabilities,” *IEEE Transactions on Plasma Science*, vol. 42, no. 10, pp. 2656–2657, 2014.

[12]M. J. Sekerak, B. W. Longmier, A. D. Gallimore, D. L. Brown, R. R. Hofer, and J. E. Polk, “Azimuthal spoke propagation in hall effect thrusters,” *IEEE Transactions on Plasma Science*, vol. 43, no. 1, pp. 72–85, 2015.

[13]M. Cappelli, Y. Raitses, and I. Kaganovich, “Coherent structures in plasmas relevant to electric propulsion,” tech. rep., Board of Trustees of the Leland Stanford Junior University Palo Alto United States, 2016.

[14]N. Hyatt, “Hall effect thruster characterization through potential, magnetic, and optical measurements,” in *55th AIAA Aerospace Sciences Meeting*, p. 0169, 2017.

[15]S. Mazouffre, L. Grimaud, S. Tsikata, K. Matyash, and R. Schneider, “Investigation of rotating spoke instabilities in a wall-less hall thruster. part i: Experiments,” in *35th International Electric Propulsion Conference*, 2017.

[16]A. Anders, P. Ni, and A. Rauch, “Drifting localization of ionization runaway: Unraveling the nature of anomalous transport in high power impulse magnetron sputtering,” *Journal of Applied Physics*, vol. 111, no. 5, p. 053304, 2012.

[17]J. Winter, A. Hecimovic, T. De los Arcos, M. Böke, and V. Schulz-von der Gathen, “Instabilities in high-power impulse magnetron plasmas: from stochasticity to periodicity,” *Journal of Physics D: Applied Physics*, vol. 46, no. 8, p. 084007, 2013.

[18]A. Hecimovic, V. Schulz-von der Gathen, M. Böke, A. von Keudell, and J. Winter, “Spoke transitions in hipims discharges,” *Plasma Sources Science and Technology*, vol. 24, no. 4, p. 045005, 2015.

[19]P. Poolcharuansin, F. L. Estrin, and J. W. Bradley, “The use of segmented cathodes to determine the spoke current density distribution in high power impulse magnetron sputtering plasmas,” *Journal of Applied Physics*, vol. 117, no. 16, p. 163304, 2015.

[20]A. Anders and Y. Yang, “Direct observation of spoke evolution in magnetron sputtering,” *Applied Physics Letters*, vol. 111, no. 6, p. 064103, 2017.

[21]A. Hecimovic, N. Britun, S. Konstantinidis, and R. Snyders, “Sputtering process in the presence of plasma self-organization,” *Applied Physics Letters*, vol. 110, no. 1, p. 014103, 2017.

[22]M. Panjan and A. Anders, “Plasma potential of a moving ionization zone in dc magnetron sputtering,” *Journal of Applied Physics*, vol. 121, no. 6, p. 063302, 2017.

[23]J. Hnilica, P. Klein, M. Šlapanská, M. Fekete, and P. Vasina, “Effect of magnetic field on spoke behaviour in hipims plasma,” *Journal of Physics D: Applied Physics*, 2018.

[24]A. Ehiasarian, A. Hecimovic, T. De Los Arcos, R. New, V. Schulz-Von Der Gathen, M. Böke, and J. Winter, “High power impulse magnetron sputtering discharges: Instabilities and plasma self-organization,” *Applied Physics Letters*, vol. 100, no. 11, p. 114101, 2012.

[25]N. Brenning, D. Lundin, T. Minea, C. Costin, and C. Vitelaru, “Spokes and charged particle transport in hipims magnetrons,” *Journal of Physics D: Applied Physics*, vol. 46, no. 8, p. 084005, 2013.

[26]K. Thomassen, “Turbulent diffusion in a penning-type discharge,” *The Physics of Fluids*, vol. 9, no. 9, pp. 1836–1842, 1966.

[27]Y. Sakawa, C. Joshi, P. Kaw, F. Chen, and V. Jain, “Excitation of the modified simon–hoh instability in an electron beam produced plasma,” *Physics of Fluids B: Plasma Physics*, vol. 5, no. 6, pp. 1681–1694, 1993.

[28]Y. Raitses, I. Kaganovich, and A. Smolyakov, “Effects of the gas pressure on low frequency oscillations in e â b discharges,” in *Proceedings of the Joint Conference of 30th ISTS, 34th IEPC, and 6th NSAT*, 2015.

[29]G. Janes, J. Dotson, and T. Wilson, “Electrostatic acceleration of neutral plasmas - momentum transfer through magnetic fields,” tech. rep., Avco Corp. Avco-Everett Research Lab., Everett, Mass., 1962.

[30]Y. Raitses and N. J. Fisch, “Parametric investigations of a nonconventional hall thruster,” *Physics of Plasmas*, vol. 8, no. 5, pp. 2579–2586, 2001.

[31]H. Alfvén, “On the origin of the solar system,” *Quarterly Journal of the Royal Astronomical Society*, vol. 8, p. 215, 1967.

[32]J.-P. Boeuf and B. Chaudhury, “Rotating instability in low-temperature magnetized plasmas,” *Physical review letters*, vol. 111, no. 15, p. 155005, 2013.

[33] J.-P. Boeuf, “Rotating structures in low temperature magnetized plasmasinsight from particle simulations,” *Frontiers in Physics*, vol. 2, p. 74, 2014.

[34] D. Escobar Anton and E. Ahedo, “Analysing the azimuthal spoke oscillation of hall thrusters via numerical simulation,” in *50th AIAA/ASME/SAE/ASEE Joint Propulsion Conference*, p. 3512, 2014.

[35] J. A. Carlsson, I. D. Kaganovich, A. V. Khrabrov, A. Smolyakov, D. Sydorenko, and Y. Raitses, “Multi-dimensional kinetic simulations of instabilities and transport in exb devices,” in *Plasma Sciences (ICOPS), 2015 IEEE International Conference on*, pp. 1–1, IEEE, 2015.

[36] D. Escobar and E. Ahedo, “Global stability analysis of azimuthal oscillations in hall thrusters,” *IEEE Transactions on Plasma Science*, vol. 43, no. 1, pp. 149–157, 2015.

[37] D. Escobar and E. Ahedo, “Low frequency azimuthal stability of the ionization region of the hall thruster discharge. ii. global analysis,” *Physics of Plasmas*, vol. 22, no. 10, p. 102114, 2015.

[38] J. Carlsson, I. Kaganovich, A. Powis, Y. Raitses, I. Romadanov, and A. Smolyakov, “Particle-in-cell simulations of anomalous transport in a penning discharge,” *arXiv preprint arXiv:1711.09790*, 2017.

[39] J. Carlsson, I. Kaganovich, A. Powis, Y. Raitses, I. Romadanov, and A. Smolyakov, “Particle-in-cell simulations of anomalous transport in a penning discharge,” *Physics of Plasmas*, vol. 25, no. 6, p. 061201, 2018.

[40] K. Matyash, R. Schneider, O. Kalentev, Y. Raitses, and N. Fisch, “Numerical investigations of a cylindrical hall thruster,” *arXiv preprint arXiv:1208.4151*, 2012.

[41] F. Taccogna and P. Minelli, “Three-dimensional fully kinetic particle-in-cell model of hall-effect thruster,” in *International Electric Propulsion Conference*, 2011.

[42] F. Taccogna, P. Minelli, M. Capitelli, and S. Longo, “Physics of hall-effect thruster by particle model,” in *AIP conference proceedings*, vol. 1501, pp. 1390–1399, AIP, 2012.

[43] K. Matyash and R. Schneider, “Particle in cell simulation of plasma thrusters,” in *Pulsed Power Conference (PPC), 2013 19th IEEE*, pp. 1–6, IEEE, 2013.

[44] K. Matyash, R. Schneider, S. Mazouffre, S. Tsikata, and L. Grimaud, “Rotating spoke instabilities in a wall-less hall thruster: Simulations,” *Plasma Sources Science and Technology*, vol. 28, no. 4, p. 044002, 2019.

[45] S. Mazouffre, L. Grimaud, S. Tsikata, K. Matyash, and R. Schneider, “Rotating spoke instabilities in a wall-less hall thruster: experiments,” *Plasma Sources Science and Technology*, vol. 28, no. 5, p. 054002, 2019.

[46] R. Kawashima, K. Hara, and K. Komurasaki, “Numerical analysis of azimuthal rotating spokes in a crossed-field discharge plasma,” *Plasma Sources Science and Technology*, vol. 27, no. 3, p. 035010, 2018.

[47] W. Frias, A. I. Smolyakov, I. D. Kaganovich, and Y. Raitses, “Long wavelength gradient drift instability in hall plasma devices. ii. applications,” *Physics of Plasmas*, vol. 20, no. 5, p. 052108, 2013.

[48] A. T. Powis, J. A. Carlsson, I. D. Kaganovich, Y. Raitses, and A. Smolyakov, “Scaling of spoke rotation frequency within a penning discharge,” *Physics of Plasmas*, vol. 25, no. 7, p. 072110, 2018.

[49] T. P. Hughes, R. E. Clark, and S. Y. Simon, “Three-dimensional calculations for a 4 ka, 3.5 mv, 2 microsecond injector with asymmetric power feed,” *Physical Review Special Topics-Accelerators and Beams*, vol. 2, no. 11, p. 110401, 1999.

[50] D. R. Welch, D. Rose, B. Oliver, and R. Clark, “Simulation techniques for heavy ion fusion chamber transport,” *Nuclear Instruments and Methods in Physics Research Section A: Accelerators, Spectrometers, Detectors and Associated Equipment*, vol. 464, no. 1-3, pp. 134–139, 2001.

[51] D. Welch, D. Rose, M. Cuneo, R. Campbell, and T. Mehlhorn, “Integrated simulation of the generation and transport of proton beams from laser-target interaction,” *Physics of Plasmas*, vol. 13, no. 6, p. 063105, 2006.

[52] D. Welch, D. Rose, R. Clark, C. Mostrom, W. Stygar, and R. Leeper, “Fully kinetic particle-in-cell simulations of a deuterium gas puff z pinch,” *Physical review letters*, vol. 103, no. 25, p. 255002, 2009.

[53] J. Carlsson, A. Khrabrov, I. Kaganovich, T. Sommerer, and D. Keating, “Validation and benchmarking of two particle-in-cell codes for a glow discharge,” *Plasma Sources Science and Technology*, vol. 26, no. 1, p. 014003, 2016.

[54] S. Balay, S. Abhyankar, M. F. Adams, J. Brown, P. Brune, K. Buschelman, L. Dalcin, V. Eijkhout, W. D. Gropp, D. Kaushik, M. G. Knepley, L. C. McInnes, K. Rupp, B. F. Smith, S. Zampini, H. Zhang, and H. Zhang, “PETSc Web page,” 2017. http://www.mcs.anl.gov/petsc.

[55] S. Balay, S. Abhyankar, M. F. Adams, J. Brown, P. Brune, K. Buschelman, L. Dalcin, V. Eijkhout, D. Kaushik, M. G. Knepley, D. A. May, L. C. McInnes, W. D. Gropp, K. Rupp, P. Sanan, B. F. Smith, S. Zampini, H. Zhang, and H. Zhang, “Petsc users manual,” Tech. Rep. ANL-95/11 - Revision 3.8, Argonne National Laboratory, 2017.

[56] S. Balay, W. D. Gropp, L. C. McInnes, and B. F. Smith, “Efficienct management of parallelism in object oriented numerical software libraries,” in *Modern Software Tools in Scientific Computing* (E. Arge, A. M. Bruaset, and H. P. Langtangen, eds.), pp. 163–202, Birkhauser Press, 1997.

[57] X. Li, J. Demmel, J. Gilbert, iL. Grigori, M. Shao, and I. Yamazaki, “SuperLU Users’ Guide,” Tech. Rep. LBNL-44289, Lawrence Berkeley National Laboratory, September 1999. http://crd.lbl.gov/~xiaoye/SuperLU/. Last update: August 2011.

[58] X. S. Li and J. W. Demmel, “SuperLU_DIST: A scalable distributed-memory sparse direct solver for unsymmetric linear systems,” *ACM Trans. Mathematical Software*, vol. 29, pp. 110–140, June 2003.

[59] D. Rapp and P. Englander-Golden, “Total cross sections for ionization and attachment in gases by electron impact. i. positive ionization,” *The Journal of Chemical Physics*, vol. 43, no. 5, pp. 1464–1479, 1965.

[60] A. Smolyakov, O. Chapurin, W. Frias, O. Koshkarov, I. Romadanov, T. Tang, M. Umansky, Y. Raitses, I. Kaganovich, and V. Lakhin, “Fluid theory and simulations of instabilities, turbulent transport and coherent structures in partially-magnetized plasmas of discharges,” *Plasma Physics and Controlled Fusion*, vol. 59, no. 1, p. 014041, 2016.

[61] J.-L. Vay, A. Almgren, J. Bell, L. Ge, D. Grote, M. Hogan, O. Kononenko, R. Lehe, A. Myers, C. Ng, *et al.*, “Warp-x: A new exascale computing platform for beam–plasma simulations,” *Nuclear Instruments and Methods in Physics Research Section A: Accelerators, Spectrometers, Detectors and Associated Equipment*, vol. 909, pp. 476–479, 2018.

[62]B. Wang, S. Ethier, W. Tang, K. Z. Ibrahim, K. Madduri, S. Williams, and L. Oliker, "Modern gyrokinetic particle-in-cell simulation of fusion plasmas on top supercomputers," *The International Journal of High Performance Computing Applications*, vol. 33, no. 1, pp. 169–188, 2019.

[63]A. H. Baker, R. D. Falgout, T. V. Kolev, and U. M. Yang, "Scaling hypres multigrid solvers to 100,000 cores," in *High-Performance Scientific Computing*, pp. 261–279, Springer, 2012.

[64]M. Heroux, R. Bartlett, V. H. R. Hoekstra, J. Hu, T. Kolda, R. Lehoucq, K. Long, R. Pawlowski, E. Phipps, A. Salinger, H. Thornquist, R. Tuminaro, J. Willenbring, and A. Williams, "An Overview of Trilinos," Tech. Rep. SAND2003-2927, Sandia National Laboratories, 2003.

[65]J.-P. Boeuf and L. Garrigues, "E× b electron drift instability in hall thrusters: Particle-in-cell simulations vs. theory," *Physics of Plasmas*, vol. 25, no. 6, p. 061204, 2018.

[66]J. P. Boris, "Relativistic plasma simulation-optimization of a hybrid code," in *Proc. Fourth Conf. Num. Sim. Plasmas, Naval Res. Lab, Wash. DC*, pp. 3–67, 1970.

[67]M. Saito and M. Matsumoto, "A prng specialized in double precision floating point numbers using an affine transition," in *Monte Carlo and Quasi-Monte Carlo Methods 2008*, pp. 589–602, Springer, 2009.